Available online at www.sciencedirect.com

ScienceDirect

journal homepage: www.elsevier.com/locate/he

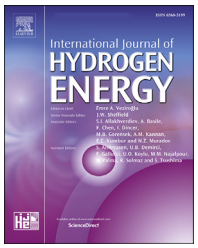

Thermochemical oxygen pumping for improved hydrogen production in solar redox cycles

Stefan Brendelberger [a,*,1], *Josua Vieten* [a,b,1], *Martin Roeb* [a], *Christian Sattler* [a,b]

[a] *Institute of Solar Research, Deutsches Zentrum für Luft- und Raumfahrt (DLR)/German Aerospace Center, Linder Höhe, 51147, Köln, Germany*

[b] *Institute of Power Engineering, Professorship of Solar Fuel production, TU Dresden, 01062 Dresden, Germany*

ARTICLE INFO

Article history:
Received 21 September 2018
Received in revised form
6 December 2018
Accepted 19 December 2018
Available online 14 January 2019

Keywords:
Oxygen pumping
Thermochemical cycles
Solar fuels
Perovskites
Thermochemical pump

ABSTRACT

Solar thermochemical cycles are promising processes for the efficient production of renewable hydrogen at large scale. One area for process optimization is the high temperature reduction step. The oxygen released during this step has to be removed from the reactor in order to increase the reduction extent of the redox material. If low partial pressures of oxygen are required, the removal of oxygen can result in a significant energy penalty for the process. Two options for oxygen removal are mainly considered so far: the use of sweep gas and vacuum pumping. Here, a third promising option is discussed - thermochemical oxygen pumping. This approach shows large energy saving potentials especially at low partial pressures of oxygen. In this study, the interaction between splitting material and pumping material is theoretically analyzed for the conditions of a demonstration campaign previously published. The presented model approach is able to capture the main mechanisms of the interaction between the two materials and the gas phase and provides predictions of the thermochemical oxygen pumping effect on the reduction extent of the splitting material. A parametric study shows the importance of the optimization of the relative material amounts. Furthermore, the influence of using different perovskite materials on the energy consumption of such a process is addressed in a more generic thermodynamic analysis. The results indicate, that by using perovskite-based redox materials, the lower limit of oxygen partial pressures for solar thermochemical cycles from an energy demand perspective might be pushed well below 10^{-10} bar. At low oxygen partial pressures, thermochemical pumps seem to be far more efficient than mechanical pumps, and their efficiency can be further improved by recovering the heat released during the oxidation of the pumping material.

* *Corresponding author.*
E-mail address: Stefan.Brendelberger@dlr.de (S. Brendelberger).

[1] The authors contributed equally to the manuscript.

https://doi.org/10.1016/j.ijhydene.2018.12.135

Introduction

Several paths are investigated for the renewable production of hydrogen using solar energy [1,2]. One path with a promising efficiency potential of large scale plants are solar thermochemical redox cycles. Concentrated solar radiation is used to drive an endothermic reduction reaction of a redox material, which in a second step splits water to obtain hydrogen. Alternatively, also carbon dioxide can be processed to open the path for syngas production and thereby the production of liquid hydrocarbons as renewable fuels. Since an intermediate conversion step to electricity is avoided and thermal energy is directly transferred into chemical energy, the theoretical efficiencies are very attractive [1]. Therefore, in the last years several of these redox cycles have been investigated in detail [3–10] and especially processes based on ceria as redox material have progressed significantly [11–13]. Different concepts have been theoretically analyzed [14–18,40] and reactors and even complete plants have been tested at pilot scale [19,20]. During these experimental campaigns, significant reactor efficiencies have been demonstrated in the range of 5% [12]. Nevertheless, several challenges have to be solved before these processes can become economically attractive.

The efforts in optimizing the concepts, materials, component designs and operation parameters are continued. One area with significant optimization potential is the parasitic energy demand for maintaining low oxygen partial pressures during the reduction of the redox material. In several studies it has been shown that especially for low oxygen partial pressures the use of a sweep gas for the removal of oxygen during the reduction leads to prohibitively large parasitic energy costs [14,21–24]. The energy demand is slightly relaxed if vacuum pumps are used for the oxygen removal. Down to pressures of about 1 mbar they seem to be the most promising solution so far [24]. Still, oxygen partial pressures of less than 1 mbar are targeted to increase the thermodynamic efficiency potential of the process. One new way for efficient oxygen removal during the reduction step has been proposed and was lately demonstrated by the authors in a proof of concept campaign: thermochemical oxygen pumping (see Fig. 1) [24,25].

A thermochemical oxygen pump avoids the efficiency drop of mechanical pumps at low pressures related to the large volumetric flow rates. It makes use of a second redox material that is applied to absorb the oxygen which is released from the first (water splitting) redox material. The thermodynamic requirements are different for the two redox materials since the material used for the oxygen pumping does not need to be able to split water. Therefore, materials with lower oxygen affinity can be used. As a consequence these materials can be reduced at significantly lower temperatures and higher oxygen partial pressures. By lowering the temperature the thermodynamic equilibrium can be shifted to higher oxygen partial pressures and the reduced material can be used to absorb oxygen from the surrounding atmosphere. If a reactor containing this reduced "pumping" material is coupled to a reactor containing the redox material for water splitting, the pumping material can be used to absorb the oxygen and lower the oxygen partial pressure during the reduction step of the splitting material. A theoretical analysis has shown that for low oxygen partial pressures (<1 mbar) the energy demand per removed mol of oxygen for cycling a pumping material between the reduction temperature and the oxygen absorbing temperature can be several orders of magnitude smaller than the corresponding energy demand of a mechanical vacuum pump. This analysis has been done exemplarily for cobalt oxide. The energy demand of such Co_3O_4/CoO-based oxygen pumping, for instance, is significantly lower than when using mechanical pumps at oxygen partial pressures lower than approx. 1 mbar [24]. The thermodynamics of this material suggest that it can be oxidized at significantly lower oxygen pressures when a lower oxidation temperature is chosen. However, the kinetics of the oxidation reaction may become a

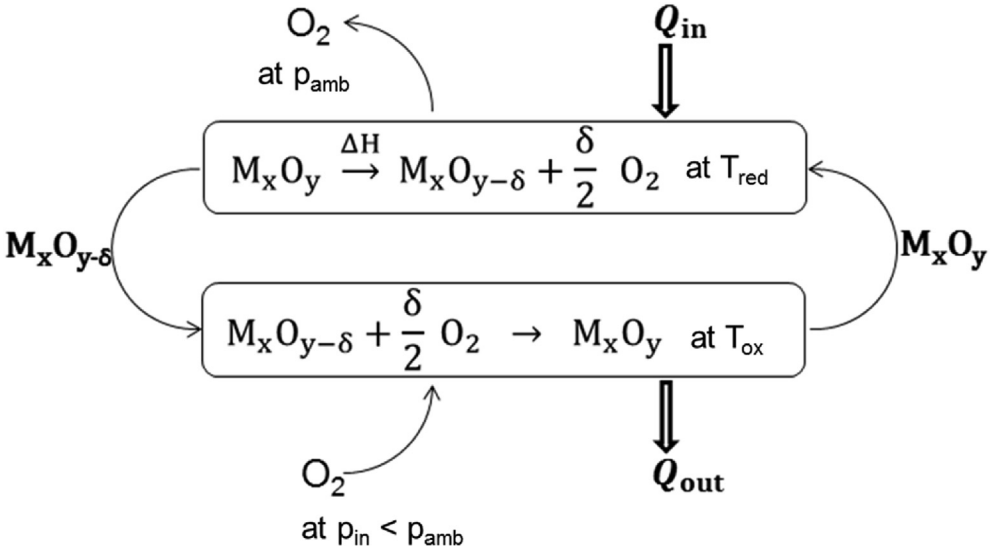

Fig. 1 – Schematic of the working principle of a thermochemical oxygen pump (adapted from Ref. [24]). Oxygen is absorbed at a low oxygen partial pressure (p_{in}) and released at a high oxygen partial pressure (p_{amb}) using a redox material in a temperature swing cycle.

limiting factor in the practical application, as the reaction involving a phase transition and re-arrangement of the crystal structure takes several minutes even in air at high temperature [26]. Among the perovskites, materials are expected which have attractive thermodynamics as well as kinetics. In an experimental campaign conducted by the authors, oxygen pumping for thermochemical cycles was demonstrated lately for $SrFeO_{3-\delta}$ as a pumping material [25]. In the study presented here, the experiments of the demonstration campaign are analyzed theoretically. Thereto a model of the experimental setting is developed with which further parametric studies can be conducted. In addition, the energy efficiency of perovskites used for oxygen pumping in general is investigated.

Theoretical analysis of demonstration campaign

In order to better understand the characteristics of the system used in the demonstration campaign presented by Brendelberger et al. [25] and in order to predict its behavior at other operational conditions, a system model is introduced. While the system used in the experiment is described in detail in Ref. [25] here a short summary of the main aspects is given.

The experimental campaign was conducted to demonstrate thermochemical oxygen pumping for redox cycles. Therefore an experimental setup (see Fig. 2) was constructed using two furnaces and a vacuum tight tube arrangement connecting ceramic reaction tubes in both furnaces. One of the furnaces contained the splitting material (SM) ceria – a redox material able to perform water and carbon dioxide splitting – while the second furnace contained a crucible holding granules of the redox material $SrFeO_{3-\delta}$ as an oxygen absorber and hence oxygen pumping material (PM). $SrFeO_{3-\delta}$ is used as it showed promising results in previous oxygen pumping experiments.

A sequence of experimental steps allows heating up the SM at reduced total pressure while being connected to the reduced PM kept at a lower temperature. While the SM heats up, it releases oxygen which is partially absorbed by the PM. At the end of the reduction step the heating of the SM is stopped and the furnace containing the PM is disconnected from the rest of the setup by closing a valve. After the SM has cooled down it is re-oxidized using a stream of nitrogen with a predefined oxygen concentration. By monitoring the oxygen concentration of the gas stream after leaving the furnace with the SM the absorbed amount of oxygen is determined and from this the previous reduction extent of the SM is deduced. The experiment was run for several settings with different mechanical evacuation durations and hence pressures at the beginning of the heating step and different masses of the PM. In the campaign it was shown that by using a PM in such a system, the reduction extent of the SM can be increased. In the following analysis the experimental results are compared to results obtained by a model considering the two materials at different temperatures and the connecting gas phase.

Model approach description

The model was developed in Python 3.6 to describe the distribution of oxygen in a system comprising the splitting material, the pumping material and a connecting gas phase, where both solid phases can exchange oxygen with the gas phase. The model makes use of several simplifying assumptions in a lumped description of the conservation of mass. It is assumed, that each redox material is in thermodynamic equilibrium with its surrounding gas phase at each point of the cycle. This refers primarily to the reduction extent of both materials. It is assumed that the temperatures of the redox materials are equal to the thermocouple readings in the two furnaces. The gas phases in the two reaction spaces are connected at the beginning of the cycle and disconnected after the heating phase. Each gas phase is modeled as an ideal gas containing two species: oxygen and nitrogen. Since the two furnaces are at different temperatures and a large share of the connecting tubes is at ambient temperature the average gas temperature is calculated as the mean temperature of the two furnaces and ambient temperature weighted by the length of the tubes in the furnaces and by the length of the tubes exposed to ambient conditions.

In this study, the terms reduction extent and non-stoichiometry are used equivalently, as the non-stoichiometry δ is directly proportional to the degree of reduction exhibited in ceria, $SrFeO_{3-\delta}$, and similar perovskites with the general composition $AMO_{3-\delta}$. The reduction extent of ceria is described using the correlation provided by Bulfin et al. [27]. It shows good agreement with experimental reduction extents for the temperature and pressure range relevant to the experiment. Also the reduction extent as function of temperature and pressure of $SrFeO_{3-\delta}$ has been characterized experimentally [28]. Based on new experimental results, an

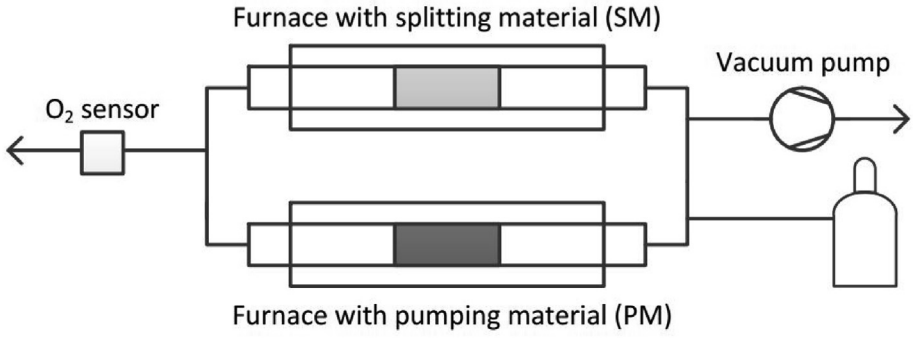

Fig. 2 – Schematic of thermochemical pumping demonstration setup (adapted from Ref. [25]).

analysis is conduced following the description presented by Bulfin et al. [27] to derive the parameters of a comparable correlation. The basic equation for both materials is defined as:

$$\left(\frac{\delta}{x-\delta}\right) = A_{ratio}\, p_{O_2}^{-n} \exp\left(\frac{-\Delta E}{RT}\right), \quad (1)$$

with the reduction extent δ and the partial pressure of oxygen p_{O_2} given in bar. The other parameters are obtained by fitting the model to the experimental data (see in Table 1).

The relation between the fitting parameters and physical meaningful characteristics is controversial since for example the notation would assume a constant reaction enthalpy which was experimentally disproved. Nevertheless, since the correlation is able to describe well the reduction extent as function of temperature and partial pressure of oxygen, it is used in the following analysis. For ceria this was shown in Ref. [27] and for $SrFeO_{3-\delta}$ it can be seen in Fig. 3. For $SrFeO_{3-\delta}$, a significant initial non-stoichiometry is present even at 400 °C in air, which is not considered further in this study, as only the change in non-stoichiometry $\Delta\delta$, is required which corresponds to the amount of oxygen absorbed and released. For ceria, $\Delta\delta$ and δ are assumed to be equivalent, as the equilibrium amount of vacancies in the ceria lattice is negligible at room temperature in air.

Since gas leakage can be observed in the experimental setup it is also included in the model. The leakage is experimentally quantified during isothermal phases by observing the pressure change over time. It is assumed, that the gas entering the setup consists of 80% nitrogen and 20% oxygen. Further, it is assumed that the leakage is constant throughout the cycle.

Modelling results and discussion

The model is validated using the experimental data published in Ref. [25]. For the comparison of the model with experimental results the equilibrium conditions for each temperature value during the heating and cooling cycle are calculated. As starting point the start of the heating phase is used. The pressure measured at this point is used as starting value for the simulation. It is assumed that the gas phase at this point consists mainly of oxygen (due to the reduction of the PM) and the nitrogen leakage which was present after the evacuation has stopped.

In Fig. 4 the experimental total pressure evolution during one cycle can be seen and compared to simulation results. The label "Basic II" refers to experimental conditions described in Ref. [25]. In order to assess the sensitivity of the model with respect to inaccuracies in the assumptions, the parameters of the model are varied. "Basic II" is using the assumptions described above; "p_start" uses a starting total pressure increased by 20%; "T_gas" assumes that only 80% of the tube length in the furnace is at the furnace temperature and 20% is at ambient temperature (recognizing the temperature distribution within the furnace) leading to a lower average temperature of the gas; "High Leakage" uses an increased leakage rate (by 10%) during the heating phase since part of the leakage is attributed to the connections of the tube element containing the PM. The pressure uncertainties were chosen based on the pressure evolution results which showed a rapid

Table 1 – Parameters for reduction extent calculation.

Parameter	SM – Ceria	PM - $SrFeO_{3-\delta}$
x	0.35	0.3
A_{ratio}	8700	190
n	0.217	0.27
ΔE (kJ mol^{-1})	195.6	49.7

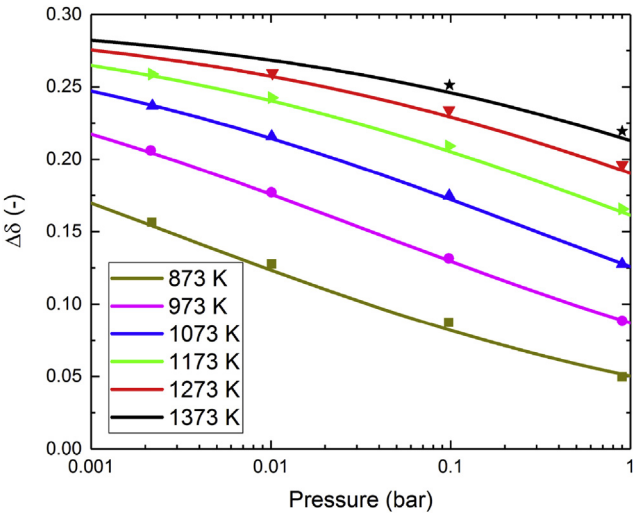

Fig. 3 – Change in Reduction extent of $SrFeO_{3-\delta}$ $\Delta\delta$ as function of the pressure at different temperatures. The points are experimental data and the lines are obtained by the correlation (Eq. (1)). The absolute non-stoichiometry δ can be derived from the $\Delta\delta$ value by adding the initial non-stoichiometry at a reference point.

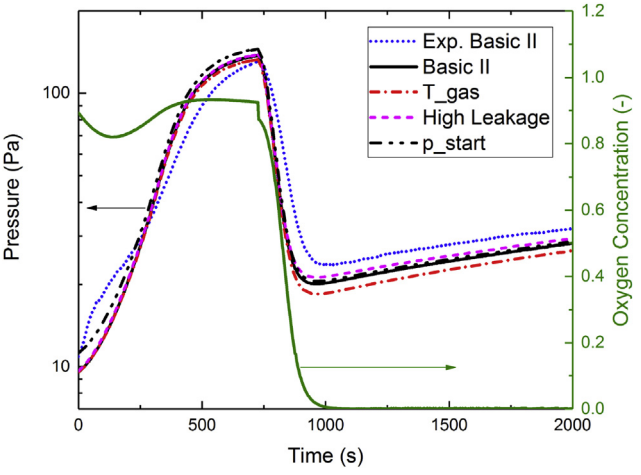

Fig. 4 – Variation of pressure during the experiment. The pressure peak coincides with the end of the heating phase. Experimental data is given as well as the results from the model with varying assumptions. In addition the model oxygen concentration is given.

relative change at the beginning (related to p_start) and a slow but steady relative increase at the end (related to "High Leakage").

As can be seen the model shows in general a good agreement with the experimental data. Discrepancies can be noticed especially at the beginning of the heating phase and during the cooling phase. The variations of the model lead to a qualitatively similar behavior and small quantitative deviations. Two effects can be identified: the oxygen release and absorption happen at a slower rate than the model predicts and the total pressure stays at a lower level in the cooling phase. One plausible explanation for the smaller pressure gradients is that the thermocouple in the furnace changes the temperature faster than the SM in the reaction tube. Causes for the lower total pressure during the cooling phase might be a higher mean temperature of the gas then obtained with the assumptions used in the model and larger leakage flows during the heating phase since several tubes are disconnected after this phase.

In a next step the comparison between experimental results and model predictions is extended to other experimental settings. The results can be seen in Fig. 5. Also for the other experimental conditions good agreement between simulation and experiment are observed. The deviations are similar to what is discussed in the context to Fig. 4.

So far the comparison focused on the total pressure - a value recorded throughout the experiment. The actual value of interest is the reduction extent of the SM during the cycle. Since in the experiment this value is measured only after the end of the cooling phase, the model values are taken for comparison at the same point in time. The reduction extent shows changes in the order of 1% when the simulations conditions are varied as described above for the sensitivity analysis. The simulation results and experimental values are depicted in Fig. 6. The simulation results show a good agreement with the trends of the experimental values when changing the duration of the evacuation and the mass of the PM. The quantitative analysis shows that a discrepancy between the simulation results and the experimental findings

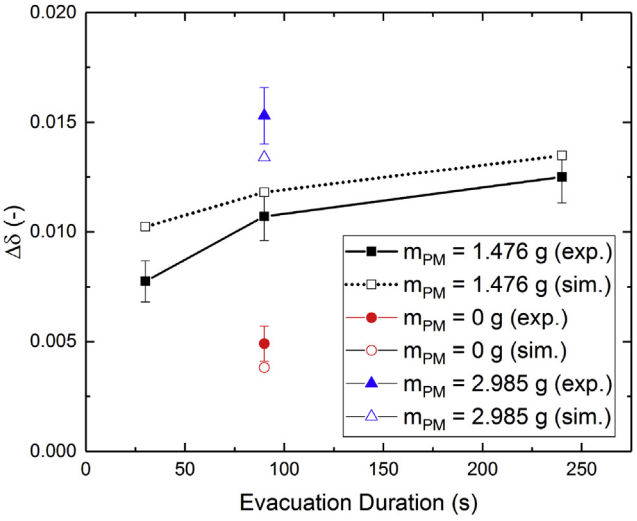

Fig. 6 – Change of reduction extent for the re-oxidation of the SM after the cooling phase.

remains but taking the simplifying assumptions of the model into account the accuracy level is rather better than expected.

Overall, the model captures the main mechanisms involved and is able to predict the change in pressure and more importantly the resulting change in reduction extend with reasonable accuracy. This encourages the application of the model for the prediction of the usage of a PM in combination with a SM for different setups and operational conditions. One example is the analysis of variations in starting pressure and molar ratios between PM and SM. The results of the simulations are shown in Fig. 7. In this simulation, leakage was omitted. In the experimental settings described above the molar ratios n_{PM}/n_{SM} varied between 0 and 0.6 and showed a strong increase in reduction extent with larger amounts of the PM. Fig. 7 shows that a saturation effect can be observed such that for pressures down to 1 Pa molar ratios above 10 have

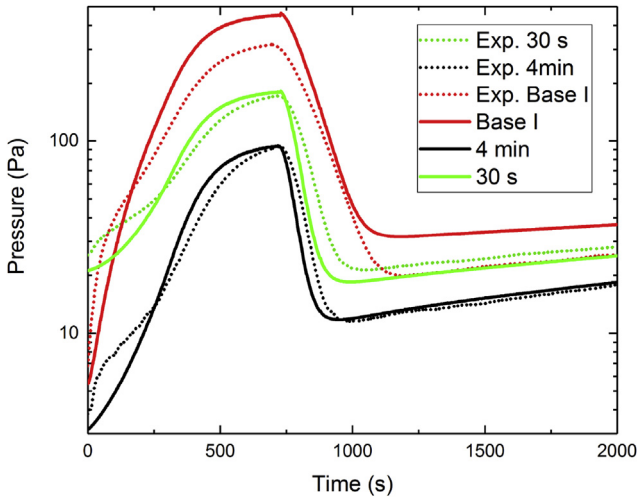

Fig. 5 – Pressure evolution for different experimental conditions and model predictions.

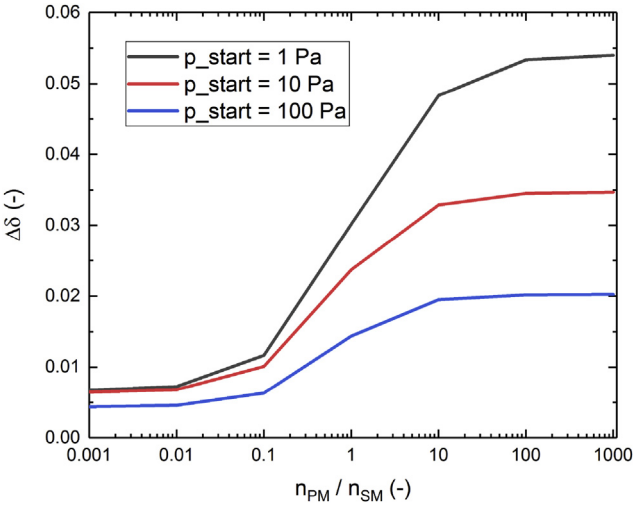

Fig. 7 – Simulation results of parameter variation for starting pressure and molar ratio.

only a limited positive effect. On the other side, for molar rations below 0.1 a positive effect is hardly noticeable.

Theoretical energy uptake of perovskite-based oxygen pumps

After the theoretical analysis of the experimental demonstration campaign and the discussion of the used model to predict the pressure evolution and reduction extent for different conditions, it is worth looking at the energetics of the process and materials-dependent process parameters. Our thermodynamic model in the previous section is in good agreement with the experimentally determined δ values, however, it relies on the availability of experimental data in this particular range of δ. Other materials may be suitable to reach lower oxygen partial pressures than demonstrated in the experimental campaign [29,30]. In the following, we therefore analyse the potential of thermochemical pumps based on different materials over a large range of oxygen partial pressures, which is beyond the experimental study. Based on theoretical data, it is possible to conduct a first study on different perovskite oxides and their energy uptake for oxygen pumping. Due to the simplifications and assumptions made, the accuracy of the model presented in the following is lower than the accuracy of the empirically based model used in the previous section, but it allows a good estimate of the redox energetics for conditions beyond the scope of our experiments.

Methodology

Within the experimental study and demonstration experiments, we have applied an empirical model to fit the changes of the redox enthalpy in dependence of the temperature and oxygen partial pressure. This, however, is only possible for materials with available experimental data. In the following, we use a model based on theoretical data to estimate the energy uptake of the process. Existing values for redox enthalpies ΔH for the complete reduction from perovskite to brownmillerite calculated via density functional theory (DFT) have been taken from *The Materials Project*, and it has been assumed that those are temperature-independent in first approximation [31–33]. The heat capacities of these perovskites were approximated based on the heat capacity of $SrFeO_{2.50}$ using a temperature-independent value of $C_p = 120\ JK^{-1}mol^{-1}$ (per mol of redox material) based on the literature [34]. This simplification introduces some errors, especially at low temperatures (<600–800 K) and if second order phase transitions are present, but it serves as a good approximation to estimate the energy uptake of such processes. Moreover, all perovskites have the same heat capacities in our model, as expected according to the Debye model for equal structures with the same amount of atoms for $T \to \infty$. The redox entropy change ΔS is dependent on the non-stoichiometry δ and consists of the following contributions:

$$\Delta S(\delta) = s_O + \Delta s_{con}(\delta) + \Delta s_{vib}(\delta) \quad (2)$$

with the partial molar entropy of oxygen gas release s_O which can be calculated using the Shomate equation using coefficients for the respective temperature ranges from 100–700 K and 700–2000 K [35], the vibrational entropy change Δs_{vib}, which is zero in our case according to the Debye model as dC_p/dT is zero [36], and the configurational entropy, which can be calculated according to Bulfin et al. using a dilute species model [29,37].

$$\Delta s_{con}(\delta) = \frac{1}{\delta_m} \cdot \frac{a}{2} \cdot R \cdot (\ln(\delta_m - \delta) - \ln \delta) \quad (3)$$

where the maximum non-stoichiometry in $ABO_{3-\delta}$ perovskites $\delta_m = 0.5$ in our case, R is the ideal gas constant, and $a = 2$ describes ideal non-interacting defect sub-lattices. It is assumed that the reduction of the perovskites occurs in ambient air ($p_{O_2} = 0.21$ bar) at elevated temperatures denoted by T_{red}. The perovskites are re-oxidized in equilibrium at a lower temperature T_{ox}, where a lower oxygen partial pressure is reached according to the Gibbs-Helmholtz equation using the values for ΔH and ΔS given above:

$$\Delta G = \Delta H - T \cdot \Delta S(\delta) + 0.5 \cdot RT \cdot \ln\left(\frac{p_{O_2}}{p_{ref}}\right) = 0 \quad (4)$$

The reference pressure $p_{ref} = 1$ bar is used. The condition $\Delta G = 0$ must be met, indicating equilibrium conditions. To do so, it is possible to either adjust the oxidation temperature while keeping δ constant, or to find a δ where equilibrium conditions are reached at constant temperature. The first approach was used by the authors in an earlier publication to calculate the energy demand of oxygen pumping using the Co_3O_4/CoO redox pair. The energy demand Q of the total process per mol of O_2 pumped can be expressed by Ref. [24].

$$Q = 2 \cdot \left(\Delta H + \frac{C_p \cdot \Delta T}{\delta_{red} - \delta_{ox}}\right) \quad (5)$$

with the non-stoichiometries δ_{red} and δ_{ox} at the reduction and oxidation step, respectively, while ΔT refers to the temperature change between the two steps. The factor 2 has to be introduced as a stoichiometric coefficient to calculate the energy demand per mol of diatomic O_2. Theoretical redox enthalpies of $SrFeO_3$ (84.6 kJ/mol_O) and $SrMnO_3$ (170.3 kJ/mol_O) are used to calculate the air separation process with reduction at $T_{red} = 800\ ^\circ C$ in air.

Within this study, the state of the chemical equilibrium is calculated under different conditions defined by the oxygen partial pressure and temperature values. The energy contributions necessary to reduce the material (sensible heat and redox enthalpy) are added to yield the total energy consumption to operate one redox cycle per mol of oxygen released. These can be lowered by assuming a certain extent of solid-solid heat recovery.

Results and discussion

If the oxidation temperature is kept constant, different non-stoichiometries δ are achieved depending on the material and the target p_{O_2}. This means that for small changes in non-stoichiometry, a low amount of oxygen is stored per mol of redox material, and more redox material is required to reach the same effect. Therefore, the heat capacity term increases

dramatically for low oxygen partial pressures in this case, as a substantial amount of redox material has to be heated and cooled in the process.

Alternatively, if the change in non-stoichiometry δ is kept constant in order to use a constant amount of redox material per mol of oxygen released, the total energy uptake is significantly lower in most cases due to the lower sensible heat input (see Fig. 8). The oxidation temperature is now a function of the target oxygen partial pressure. A limit of $T_{red} > 250$ °C is used due to kinetic limitations suggesting significantly increased reaction times at lower temperatures [33]. This induces a limiting p_{O_2} for each material which cannot be undercut. It is evident that a thermochemical pump based on perovskites is more efficient than a mechanical pump at oxygen partial pressures in the sub-millibar range. As opposed to the Co_3O_4/CoO redox pair, where the chemical and sensible heat input are in the same order of magnitude, the heat input of perovskite-based thermochemical pumps is mainly governed by the latent heat demand. The chemical energy required to partially reduce these oxides is quite low, especially in the case of $SrFeO_{3-\delta}$. This implies that using heat exchangers to recover the latent heat will significantly improve the efficiency of these thermochemical pumps, as shown in Fig. 9 for different heat recovery efficiencies η_{hrec}. A possible heat recovery concept has been outlined by Felinks et al. with theoretical efficiencies above 50% [38,39]. With efficient heat recovery, perovskite-based oxygen pumps may surpass the efficiency of a cobalt oxide-based pump [24], while offering the advantage of reaching lower oxygen partial pressures and faster redox kinetics [26,33] while using earth-abundant materials based on strontium, iron, and manganese. These redox materials allow reaching lower oxygen partial pressures than with mechanical pumps at moderate energy inputs. While the practical realization of this concept remains challenging, perovskite-based thermochemical pumps may play an essential role in increasing the efficiency of two step solar-thermochemical cycles for fuel production through enabling the reduction of the splitting material at lower oxygen partial pressures and lower cycle times than possible using stoichiometric oxides. The increased reduction extent directly translates to a higher hydrogen yield per cycle, which corresponds to significantly decreased hydrogen production costs. Techno-economical aspects of a scaled-up process will be addressed in future studies. It is important to note that while the temperature-dependent change in the redox enthalpies and inaccuracies in the DFT calculated-values do not have a large effect on the overall energy uptake per mol of material, these uncertainties do affect the accuracy of the thermodynamic calculations and the corresponding amount of oxygen absorbed or released. Therefore, our studies are intended to give an outlook on the possibilities of this technology, but the

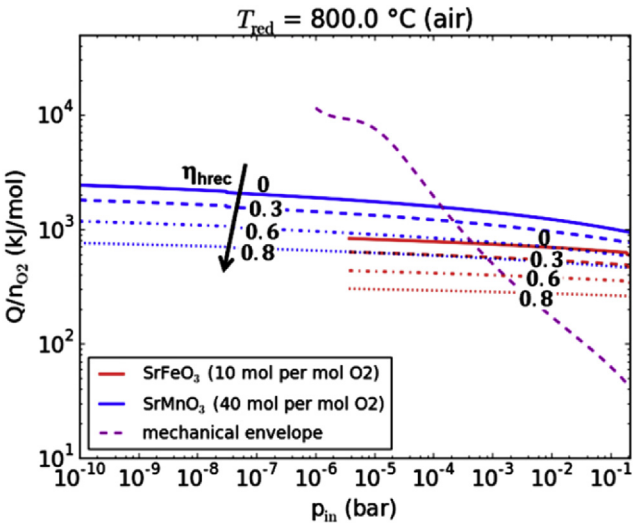

Fig. 9 – Heat input for thermochemical air separation with perovskite materials under consideration of recovery of the latent heat at an efficiency η_{hrec}. The heat recovery efficiency plays a key role in the efficiency of the whole process.

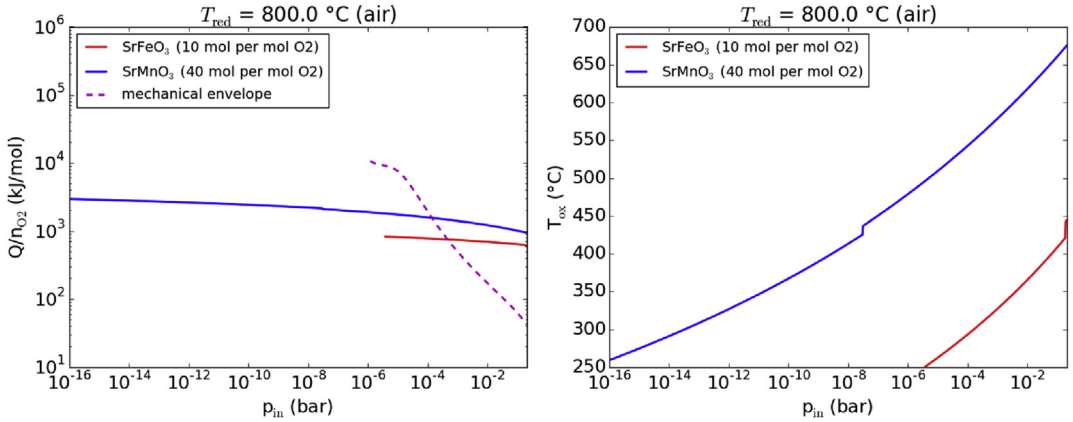

Fig. 8 – Thermochemical oxygen pumping using perovskites at constant non-stoichiometry change $\Delta\delta = 0.2$ for SrFeO3-δ and 0.05 for SrMnO3-δ with a reduction step at Tred = 800 °C in air. The graph on the left shows the energy demand for oxygen pumping, while the graph on the right depicts the oxidation temperature. The mechanical envelope is the energy demand of a mechanical vacuum pump as provided by Brendelberger et al. [24]. The steps at about 450 °C are induced due to the calculation of s_o based on the Shomate equation with different constants at T < 700 K and T > 700 K.

values have to be verified experimentally. More detailed thermodynamic models are part of ongoing studies.

Conclusions

In previous publications the authors introduced the concept of thermochemical oxygen pumps for oxygen removal during the reduction step of solar thermochemical cycles in a first conceptual study considering CoO as pumping material and presented experimental results of a demonstration campaign. Now, in this study, the concept of thermochemical oxygen pumping is further investigated by, firstly, analyzing the demonstration campaign theoretically and presenting a simple model approach that captures well the main mechanisms in the setup and as such can be used to assess the implementation of pumping material under various conditions. Secondly, the theoretical potential of perovskites applied to solar thermochemical cycles is analyzed from an energetic perspective exemplarily for 2 materials based on literature thermodynamic data: $SrFeO_3$ and $SrMnO_3$. As shown in the analysis, the advantage of oxygen pumping is especially pronounced for pressures below 1 mbar. There the required energy amount is significantly lower compared to mechanical oxygen pumps. In comparison to the performance of CoO the analyzed perovskites showed higher energy demands. Nevertheless, if efficient heat recovery strategies for the pumping material are applied perovskites might even outperform CoO. In addition CoO seems to be kinetically limited and might require long cycle times while perovskites show typically much higher reaction rates, which might be another important advantage of these materials in comparison to CoO for the application in solar thermochemical cycles.

Acknowledgement

This work has received funding from the European Union's Horizon 2020 research and innovation program under grant agreement no. 654408, it was supported by the Swiss State Secretariat for Education, Research and Innovation (SERI) under contract number 15.0330, and from the Helmholtz Association within the Virtual Institute SolarSyngas (VH-VI-509), as well as within the project DÜSOL (EFRE-0800603) which is co-funded in the Klimaschutzwettbewerb "ErneuerbareEnergien.NRW" by the state of Northrhine-Westphalia, Germany, and the European EFRE fund.

REFERENCES

[1] Steinfeld A. Solar thermochemical production of hydrogen––a review. Sol Energy 2005;78:603–15.
[2] Nakamura T. Hydrogen production from water utilizing solar heat at high temperatures. Sol Energy 1977;19:467–75.
[3] Scheffe JR, Weibel D, Steinfeld A. Lanthanum–strontium–manganese perovskites as redox materials for solar thermochemical splitting of H_2O and CO_2. Energy Fuels 2013;27:4250–7.
[4] Call F, Roeb M, Schmücker M, Bru H, Curulla-Ferre D, Sattler C, Pitz-Paal R. Thermogravimetric analysis of zirconia-doped ceria for thermochemical production of solar fuel. Am J Anal Chem 2013;4:37–45.
[5] McDaniel AH, Miller EC, Arifin D, Ambrosini A, Coker E, O'Hayre R, Chueh W, Tong J. Sr-and Mn-doped LaAlO3-δ for solar thermochemical H2 and CO production. Energy Environ Sci 2013;6:2424–8.
[6] Ezbiri M, Becattini V, Hoes M, Michalsky R, Steinfeld A. High redox capacity of Al-doped La1-xSrxMnO3-δ (0≤ x≤ 1) perovskites for splitting CO2 and H2O at Mn-enriched surfaces. ChemSusChem 2017;10(7):1517–25.
[7] Allen KM, Coker EN, Auyeung N, Klausner JF. Cobalt ferrite in YSZ for use as reactive material in solar thermochemical water and carbon dioxide splitting, Part I: material characterization. J Miner Met Mater Soc 2013;65:1670–81.
[8] Muhich C, Evanko B, Liang X, Lichty P, Arafin D, Weston KC, Musgrave CB, Weimer A. Green hydrogen production using a cobalt ferrite based hercynite solar thermal water splitting cycle. 2012.
[9] Steinfeld A. Solar hydrogen production via a two-step water-splitting thermochemical cycle based on Zn/ZnO redox reactions. Int J Hydrogen Energy 2002;27:611–9.
[10] Bulfin B, Lange M, de Oliveira L, Roeb M, Sattler C. Solar thermochemical hydrogen production using ceria zirconia solid solutions: efficiency analysis. Int J Hydrogen Energy 2016;41:19320–8.
[11] Abanades S, Flamant G. Thermochemical hydrogen production from a two-step solar-driven water-splitting cycle based on cerium oxides. Sol Energy 2006;80:1611–23.
[12] Marxer D, Furler P, Takacs M, Steinfeld A. Solar thermochemical splitting of CO2 into separate streams of CO and O2 with high selectivity, stability, conversion, and efficiency. Energy Environ Sci 2017;10:1142–9.
[13] Bhosale RR, Takalkar G, Sutar P, Kumar A, AlMomani F, Khraisheh M. A decade of ceria based solar thermochemical H2O/CO2 splitting cycle. Int J Hydrogen Energy 2018;44(1):34–60.
[14] Lapp J, Davidson JH, Lipiński W. Efficiency of two-step solar thermochemical non-stoichiometric redox cycles with heat recovery. Energy 2012;37:591–600.
[15] Bader R, Venstrom LJ, Davidson JH, Lipiński W. Thermodynamic analysis of isothermal redox cycling of ceria for solar fuel production. Energy Fuels 2013;27:5533–44.
[16] Ermanoski I, Siegel NP, Stechel EB. A new reactor concept for efficient solar-thermochemical fuel production. J Sol Energy Eng 2013;135:031002.
[17] Brendelberger S, Sattler C. Concept analysis of an indirect particle-based redox process for solar-driven H2O/CO2 splitting. Sol Energy 2015;113:158–70.
[18] Muhich CL, Blaser S, Hoes MC, Steinfeld A. Comparing the solar-to-fuel energy conversion efficiency of ceria and perovskite based thermochemical redox cycles for splitting H2O and CO2. Int J Hydrogen Energy 2018;43:18814–31.
[19] Säck JP, Breuer S, Cotelli P, Houaijia A, Lange M, Wullenkord M, Spenke C, Roeb M, Sattler C. High temperature hydrogen production: design of a 750KW demonstration plant for a two step thermochemical cycle. Sol Energy 2016;135:232–41.
[20] Koepf E, Zoller S, Luque S, Thelen M, Brendelberger S, Gonzalez-Aguilar J, Romero M, Steinfeld A. Liquid fuels from concentrated sunlight: an overview on development and integration of a 50 kW solar thermochemical reactor and high concentration solar field for the SUN-to-LIQUID project. In: SolarPACES; 2018. Morocco.
[21] Ermanoski I, Siegel NP, Stechel EB. A new reactor concept for efficient solar-thermochemical fuel production. J Sol Energy Eng 2013;135. 031002-031002-031010.

[22] Lin M, Haussener S. Solar fuel processing efficiency for ceria redox cycling using alternative oxygen partial pressure reduction methods. Energy 2015;88:667–79.
[23] Brendelberger S, Roeb M, Lange M, Sattler C. Counter flow sweep gas demand for the ceria redox cycle. Sol Energy 2015;122:1011–22.
[24] Brendelberger S, von Storch H, Bulfin B, Sattler C. Vacuum pumping options for application in solar thermochemical redox cycles – assessment of mechanical-, jet- and thermochemical pumping systems. Sol Energy 2017;141:91–102.
[25] Brendelberger S, Vieten J, Juttu Vidyasagar M, Roeb M, Sattler C. Demonstration of thermochemical oxygen pumping for atmosphere control in reduction reactions. Sol Energy 2018;170:273–9.
[26] Block T, Schmücker M. Metal oxides for thermochemical energy storage: a comparison of several metal oxide systems. Sol Energy 2016;126:195–207.
[27] Bulfin B, Lowe AJ, Keogh KA, Murphy BE, Lübben O, Krasnikov SA, Shvets IV. Analytical model of CeO2 oxidation and reduction. J Phys Chem C 2013;117:24129–37.
[28] Vieten J, Bulfin B, Senholdt M, Roeb M, Sattler C, Schmücker M. Redox thermodynamics and phase composition in the system SrFeO3 – δ — SrMnO3 – δ. Solid State Ionics 2017;308:149–55.
[29] Bulfin B, Vieten J, Starr DE, Azarpira A, Zachäus C, Haevecker M, Skorupska K, Schmuecker M, Roeb M, Sattler C. Redox chemistry of CaMnO3 and Ca0.8Sr0.2MnO3 oxygen storage perovskites. J Mater Chem A 2017;5:7912–9.
[30] Bulfin B, Vieten J, Agrafiotis C, Roeb M, Sattler C. Applications and limitations of two step metal oxide thermochemical redox cycles; a review. J Mater Chem A 2017;5:18951–66.
[31] Jain A, Hautier G, Ong SP, Moore CJ, Fischer CC, Persson KA, Ceder G. Formation enthalpies by mixing GGA and GGA $+$ U calculations. Phys Rev B 2011;84:045115.
[32] Jain A, Ong SP, Hautier G, Chen W, Richards WD, Dacek S, Cholia S, Gunter D, Skinner D, Ceder G, Persson KA. Commentary: the Materials Project: a materials genome approach to accelerating materials innovation. Apl Mater 2013;1:011002.
[33] Vieten J, Bulfin B, Call F, Lange M, Schmucker M, Francke A, Roeb M, Sattler C. Perovskite oxides for application in thermochemical air separation and oxygen storage. J Mater Chem 2016;4:13652–9.
[34] Haavik C, Bakken E, Norby T, Stolen S, Atake T, Tojo T. Heat capacity of SrFeO3-[small delta]; [small delta][space]= 0.50, 0.25 and 0.15 - configurational entropy of structural entities in grossly non-stoichiometric oxides. Dalton Trans 2003:361–8.
[35] Chase MW. S. National Institute of, Technology, NIST-JANAF thermochemical tables. [Washington, D.C.]; Woodbury, N.Y.: American Chemical Society ; American Institute of Physics for the National Institute of Standards and Technology; 1998.
[36] Fultz B. Vibrational thermodynamics of materials. Prog Mater Sci 2010;55:247–352.
[37] Bulfin B, Hoffmann L, de Oliveira L, Knoblauch N, Call F, Roeb M, Sattler C, Schmucker M. Statistical thermodynamics of non-stoichiometric ceria and ceria zirconia solid solutions. Phys Chem Chem Phys 2016;18:23147–54.
[38] Felinks J, Brendelberger S, Roeb M, Sattler C, Pitz-Paal R. Heat recovery concept for thermochemical processes using a solid heat transfer medium. Appl Therm Eng 2014;73:1006–13.
[39] Felinks J, Richter S, Lachmann B, Brendelberger S, Roeb M, Sattler C, Pitz-Paal R. Particle–particle heat transfer coefficient in a binary packed bed of alumina and zirconia-ceria particles. Appl Therm Eng 2016;101:101–11.
[40] Ehrhart BD, Muhich CL, Al-Shankiti I, Weimer AW. System efficiency for two-step metal oxide solar thermochemical hydrogen production – Part 1: Thermodynamic model and impact of oxidation kinetics. Int J Hydrogen Energy 26 November 2016;41(44):19881–93.